# Performance Analysis and Optimization Strategy over Cell-Free Massive MIMO in the Finite Blocklength Regime

Qingqin Xu[1(✉)], Zhong Li[1], Teng Wu[1], and Jie Zeng[2]

[1] School of Communication and Information Engineering, Chongqing University of Posts and Telecommunications, Chongqing 400065, China
{s210131272,s190131188,s200131102}@stu.cqupt.edu.cn
[2] Department of Electronic Engineering, Tsinghua University, Beijing 100084, China
zengjie@tsinghua.edu.cn

**Abstract.** The sixth generation (6G) mobile networks need to meet various performance requirements such as the number of connections, latency, reliability, and energy efficiency. In particular, for the Internet of Things (IoT) scenarios with short packet transmission, it is necessary to analyze and optimize various performances while achieving massive connections. In addition, practical constraints (such as imperfect channel state information, limitations of classical Shannon's capacity, inter-cell interference, massive user interference, etc.) further aggravate the difficulties of theoretical analysis and performance improvement. We propose a performance analysis and optimization strategy for short packet transmission systems based on cell-free massive multiple-input multiple-output (CF mMIMO), which points out the idea of improving system performance with large-scale connections under practical constraints. Furthermore, with the combination of simultaneous wireless information and power transfer (SWIPT) technology and finite blocklength (FBL) information theory, we derive the closed-form expressions of downlink signal-to-interference-plus-noise ratio (SINR), achievable data rate, and energy collected based on CF mMIMO. Simulation results verify the effectiveness of the proposed strategy, which is also expected to support massive ultra-reliable and low latency communications (mURLLC) with ultra-high energy efficiency or spectral efficiency in the future.

**Keywords:** Cell-free massive multiple-input multiple-output (CF mMIMO) · Finite blocklength (FBL) · Massive ultra-reliable and low latency communications (mURLLC) · Performance analysis and optimization · Simultaneous wireless information and power transfer (SWIPT)

This work was supported by the National Natural Science Foundation of China (No. 62001264) and the Natural Science Foundation of Beijing (No. L192025).


F. Gao et al. (Eds.): ChinaCom 2022, LNICST 500, pp. 137–148, 2023.
https://doi.org/10.1007/978-3-031-34790-0_11

## 1 Introduction

From the fifth generation (5G) to the sixth generation (6G), in addition to the number of access users that need to be significantly improved, ultra-high spectral efficiency, ultra-low latency and ultra-high reliability have also become basic indicators that 6G needs to be guaranteed [7,10]. In response to these changes, new theories, methods and technologies are urgently needed for 6G.

Related research has been made by some scholars recently. Saad *et al.* [7] first proposed massive ultra-reliable and low latency communications (mURLLC) and pointed out that mURLLC covers four performance indicators: massive connections, ultra-high reliability, ultra-low latency, and scalability (e.g., ultra-high spectral efficiency, wide area coverage, etc.). Zhang *et al.* [11] analyzed the quality-of-service (QoS) for mURLLC with statistical delay. Liu *et al.* [2] optimized indicators such as the number of user accesses, latency, and reliability to achieve mURLLC. In addition, the cell-free massive multiple-input multiple-output (CF mMIMO) which has great potential to become one of the key technologies for 6G greatly reduces the user-to-base station distance in traditional cellular cells and has a strong anti-fading capability [1]. Ngo *et al.* [5] analyzed the user achievable data rate and system throughput for the first time for an uplink CF mMIMO system considering the effects of channel estimation error and power control. Nasir *et al.* [4] studied a CF mMIMO system implementing downlink ultra-reliable and low latency communications (URLLC) and optimized the system data rate and energy efficiency.

Although mURLLC, CF mMIMO and other new theories and technologies have been proposed, the related research is still in the exploration stage. There is still much room for exploration to achieve the requirements of 6G multiple performance indicators (reliability, latency, user capacity, etc.). Furthermore, for 6G key performance indicators differentiation and linkage characteristics, how to build an evaluation system to break through the bottleneck of system performance improvement and accelerate program design and simulation verification has not been solved.

The key contributions of this paper can be summarized as follows.

- A performance analysis and optimization strategy over CF mMIMO for short packet transmission is proposed for large-scale IoT scenarios, which is expected to support future mURLLC with ultra-high energy or spectral efficiency.
- Combining simultaneous wireless information and power transfer (SWIPT), we derive closed-form expressions for downlink signal-to-interference-plus-noise (SINR), achievable data rate, and energy collected with finite block-length (FBL) information theory over CF mMIMO.

The remainder of this paper is organized as follows. Section 2 describes the strategy of performance evaluation. In Sect. 3, we analyze a case of CF mMIMO. In Sect. 4, simulation results are shown and analyzed. Finally, conclusions are given in Sect. 5.

*Notations*: $\mathbb{C}^{K\times N}$ collects $K \times N$ complex-valued matrices. $\mathbb{E}(\bullet)$ denotes expectation. $(\bullet)^H$ denote transpose and conjugate. $\mathcal{CN}(0,1)$ denotes the zero-mean complex Gaussian distribution with variance 1.

## 2 System Model and Performance Evaluation

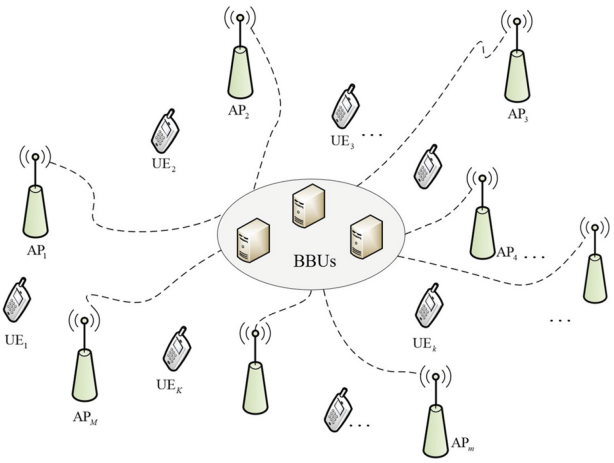


**Fig. 1.** Architecture diagram of the CF mMIMO system.

A CF mMIMO system contains $M$ access points (APs) and $K$ user equipments (UEs) as shown in Fig. 1. By deploying massive APs in a distributed manner, the spatial diversity gain is obtained, and the path loss is greatly reduced, thereby significantly improving the achievable data rate and reliability. In addition, high-performance base band units (BBUs) are used to collectively process the signals of multiple APs, which improve the number of access users and the performance of multi-user detection. Assuming that each AP or UE has a single antenna, the received signal can be modeled as

$$\mathbf{Y} = \mathbf{G}\mathbf{X} + \mathbf{Z}, \tag{1}$$

where $\mathbf{G} \in \mathbb{C}^{M\times K}$ is the channel matrix. $\mathbf{X} \in \mathbb{C}^{K\times N}$ is the transmitted signal and $N$ is the number of channel uses (CUs). $\mathbf{Y} \in \mathbb{C}^{M\times N}$ is the received signal. $\mathbf{Z} \in \mathbb{C}^{M\times N}$ is the noise at the receiver and other co-channel interference. We assume that $g_{mk}$ represents the channel coefficient between the $m$-th AP and the $k$-th UE, then the channel can be modeled as

$$g_{mk} = h_{mk}\sqrt{\beta_{mk}}, \tag{2}$$

where $h_{mk} \sim \mathcal{CN}(0,1)$ is the small-scale Rayleigh fading coefficient between the $m$-th AP and the $k$-th UE, and remains unchanged throughout the coherent interval [3]; $\beta_{mk}$ is the large-scale fading between the $m$-th AP and the $k$-th UE and considers path loss $\beta_{mk}(d_{mk}) = \min\left(1, d_{mk}^{-\alpha_{\mathrm{PL}}}\right)$ as a nonsingular bounded path loss model, which $d_{mk}$ is the distance and $\alpha_{\mathrm{PL}} > 0$ is the path loss factor. It is usually assumed that $\beta_{mk}$ is known in advance [3,5].

In light of various needs of 6G, the following describes the performance evaluation strategy based on CF mMIMO for short packet transmission, combined with FBL information theory, mainly including the following three contents.

**Analyze the Achievable Performance of CF mMIMO System Based on Practical Constraints.** In practical scenarios, it is difficult to obtain perfect channel state information (CSI) due to the time-varying channel state and limited pilot overhead. Therefore, based on the CF mMIMO system, a CSI error model need to be established first. For example, based on expressing the channel coefficients above, by using the pilot signal sent by the UE, the AP estimates the uplink channel locally [5]. The pilot signal received at the $m$-th AP can be expressed as [3,5]

$$\boldsymbol{y}_m = \sqrt{n_p P_p} \sum_{k=1}^{K} g_{mk} \boldsymbol{\varphi}_k + \boldsymbol{n}_m, \tag{3}$$

where $n_p$ is the pilot sequence length, $P_p$ is the pilot transmission power of each UE, $\varphi_k \in \mathbb{C}^{1\times n_p}$ is pilot sequence assigned to $k$-th UE, and $\|\varphi_k\|^2 = 1$. $n_m$ is the additive white Gaussian noise (AWGN) vector at the $m$-th AP, whose elements follow $\mathcal{CN}(0,1)$. Project $y_m$ in the direction of $\varphi_k^H$ to get

$$y_{mk} = \boldsymbol{y}_m \boldsymbol{\varphi}_k^H = \sqrt{n_p P_p} g_{mk} + \sqrt{n_p P_p} \sum_{\substack{k'=1 \\ k' \neq k}}^{K} \boldsymbol{\varphi}_{k'} \boldsymbol{\varphi}_k^H + n_m, \tag{4}$$

where $n_m = n_m \varphi_k^H \sim \mathcal{CN}(0,1)$. Using the minimum mean-squared error (MMSE) criterion, the estimation of channel coefficients $g_{mk}$ can be expressed as [8]

$$\hat{g}_{mk} = \frac{\mathbb{E}\left[y_{mk}^* g_{mk}\right]}{\mathbb{E}\left[\left|y_{mk}\right|^2\right]} y_{mk} = c_{mk} y_{mk}, \tag{5}$$

where $c_{mk}$ is expressed as

$$c_{mk} \triangleq \frac{\sqrt{n_p P_p}\beta_{mk}}{n_p P_p \sum\limits_{k'=1}^{K} \beta_{mk} \left|\boldsymbol{\varphi}_k^H \boldsymbol{\varphi}_{k'}\right|^2 + 1}. \tag{6}$$

The actual channel can be expressed as $g_{mk} = \hat{g}_{mk} + \tilde{g}_{mk}$, where $\tilde{g}_{mk}$ is the estimation error, due to the orthogonality of MMSE criterion [8], $\tilde{g}_{mk}$ and $\hat{g}_{mk}$ is independent of each other. Then, through the massive user access and detection scheme, the post-processing signal-to-noise ratio, achievable data rate and other performance indicators can be derived under imperfect CSI.

**Establish a Performance Evaluation System Around Indicators.** The classical Shannon's capacity is based on the assumption of infinite coding block-length, which cannot accurately describe the achievable data rate of short packet

communication. Therefore, we can use FBL information theory to model and analyze data rate and error probability. The achievable data rate $R_k$ of the $k$-th UE is [6]

$$R_k \approx C(\gamma_k) - \sqrt{\frac{V(\gamma_k)}{n'}} Q^{-1}(\varepsilon_k), \tag{7}$$

where $\varepsilon_k$ $(0 \leq \varepsilon_k < 1)$ is the decoding error probability at the $k$-th UE; $n'$ is the length of coding block; $Q^{-1}(\cdot)$ represents the inverse function of a function $Q$; $\gamma_k$ is the SINR at the $k$-th UE, $C(\gamma_k) = \log_2(1+\gamma_k)$ and $V(\gamma_k) = 1 - \frac{1}{(1+\gamma_k)^2}$. The decoding error probability $\varepsilon_k(n_d, \gamma_k)$ of the $k$-th UE is

$$\varepsilon_k(n_d, \gamma_k) \approx Q\left(\frac{C(\gamma_k) - R_k}{\sqrt{V(\gamma_k)/n'}}\right). \tag{8}$$

Furthermore, theoretical relationships between the achievable data rate and other performance indicators can be deduced.

**Optimize the Transmission Scheme for Typical Scenarios.** The performance evaluation and analysis system is beneficial for providing references for scheme design and simulation. For example, based on (7), the latency $t_{\mathrm{D}}$ and spectral efficiency $\eta_{\mathrm{SE}}$ can be expressed as

$$t_{\mathrm{D}} = \max_k \frac{D_k}{R_k}, \quad \eta_{\mathrm{SE}} = \frac{\sum_{k=1}^{K} R_k}{B_{\mathrm{total}}}, \tag{9}$$

where $D_k$ is the packet size of $k$-th user, and $B_{\mathrm{total}}$ is the total bandwidth of the system. For specific scenarios, we can optimize the performance of one or several indicators. Then, we can analyze the relationship between the achievable data rate, reliability, latency and spectral efficiency with simulation. By adjusting the parameters, the transmission scheme is further adjusted to meet the performance requirements. Because of using the CF mMIMO system that supports massive connections and considering short packet transmission, the above strategy is expected to support mURLLC with ultra-high energy efficiency or spectral efficiency in the future.

## 3 Use Case and Performance Analysis

In this section, a use case of a CF mMIMO system in Fig. 1 is introduced. Combined with SWIPT technology, we assume that each UE is equipped with information and energy receivers, and the energy collection model of each UE is generalized by using time-switching (TS) and power-splitting (PS). Each coherent interval $n_c$ ($n_c = B_c T_c$, where $B_c$ refers to coherent bandwidth and $T_c$ refers to coherent time) is divided into two orthogonal time slots, which are used for uplink pilot training and downlink SWIPT transmission respectively. The system model is shown in Fig. 2.

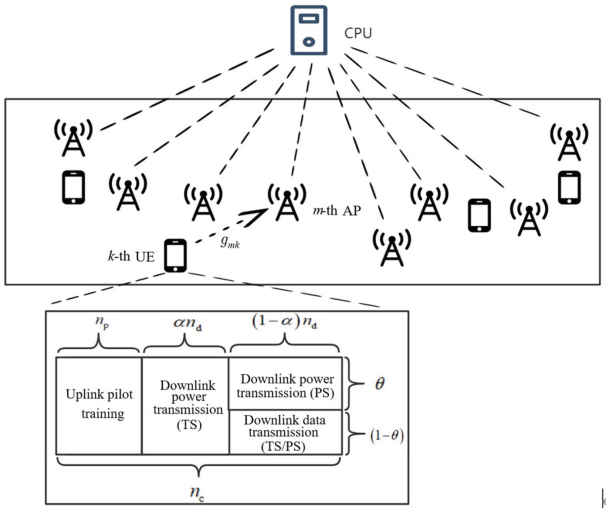


**Fig. 2.** System model of CF MIMO with SWIPT.

### 3.1 Downlink Data Transmission

Channel estimation in uplink has been done in Sect. 2. Using the joint TS-PS protocol, based on the TS factor $\alpha$ and PS factor $\theta$, the downlink SWIPT transmission phase is divided into two sub-phases. In the first downlink power transmission sub-phase, UE uses $\alpha n_d$ CUs to collect energy from AP based on TS protocol, and $n_d$ is the number of CUs used in downlink transmission phase. At this time, each UE is fully represented as an energy collection device and collects energy from the AP. In the second downlink information transmission subphase, the remaining $(1-\alpha)\, n_d$ CUs are used for downlink information transmission. If PS protocol is adopted, the received signal energy is divided into two streams, which are used for energy collection and information decoding respectively. $\tilde{n}_d \triangleq (1-\alpha)\, n_d$ indicates the blocklength of the downlink data, and the transmission signal vector $x_m^{\tilde{n}_d}$ at the $m$-th AP can be expressed as

$$\boldsymbol{x}_m^{\tilde{n}_d} = \sqrt{(1-\theta)\, P_d} \sum_{k=1}^{K} \sqrt{\eta_{mk}} \hat{g}_{mk}^{*} \boldsymbol{s}_k^{\tilde{n}_d}, \tag{10}$$

where $\boldsymbol{s}_k^{\tilde{n}_d} = \left[ s_k^{(1)}, ..., s_k^{(\tilde{n}_d)} \right]$ is the symbol vector sent to the $k$-th UE, $s_k^{(l)}, l \in \{1, ..., \tilde{n}_d\}$ is the $l$-th data symbol sent to the $k$-th UE, and $\mathbb{E}\left[ \left| s_k^{(l)} \right|^2 \right] = 1, l \in \{1, ..., \tilde{n}_d\}$. $\eta_{mk}$ is the power allocation coefficient between the $m$-th AP and the $k$-th UE, and meets the following power constraints at each AP

$$\sum_{k=1}^{K} \eta_{mk} \mathbb{E}\left[ \left| \hat{g}_{mk}^{*} \right|^2 \right] \leq 1 \;\Rightarrow\; \sum_{k=1}^{K} \eta_{mk} \rho_{mk} \leq 1, \tag{11}$$

where the expression of $\rho_{mk}$ is

$$\rho_{mk} \triangleq \mathbb{E}\left[\left|\hat{g}_{mk}^{*}\right|^{2}\right] = \sqrt{n_p P_p}\beta_{mk} c_{mk}. \tag{12}$$

Thus, the signal received by the $k$-th UE from the $M$ APs can be expressed as

$$\begin{aligned} \boldsymbol{y}_k^{\tilde{n}_d} &= \sum_{m=1}^{M} g_{mk} \boldsymbol{x}_m^{\tilde{n}_d} + n_k \\ &= \sqrt{(1-\theta) P_d} \sum_{m=1}^{M} \sum_{k'=1}^{K} \sqrt{\eta_{mk'}} g_{mk} \hat{g}_{mk'}^{*} \boldsymbol{s}_{k'}^{\tilde{n}_d} + n_k, \end{aligned} \tag{13}$$

where $n_k \sim \mathcal{CN}(0,1)$ represents the AWGN at the $k$-th UE. Further, the received signal $\boldsymbol{y}_k^{\tilde{n}_d}$ in (13) can be rewritten as

$$\begin{aligned} \boldsymbol{y}_k^{\tilde{n}_d} =& \sqrt{(1-\theta) P_d} \sum_{m=1}^{M} \sqrt{\eta_{mk}} g_{mk} \hat{g}_{mk}^{*} \boldsymbol{s}_k^{\tilde{n}_d} \\ &+ \sqrt{(1-\theta) P_d} \sum_{m=1}^{M} \sum_{\substack{k'=1 \\ k' \neq k}}^{K} \sqrt{\eta_{mk'}} g_{mk'} \hat{g}_{mk'}^{*} \boldsymbol{s}_{k'}^{\tilde{n}_d} + n_k, \end{aligned} \tag{14}$$

Thus, the SINR at the $k$-th UE can be expressed as [12]

$$\begin{aligned} \gamma_k =& (1-\theta) P_d \left( \sum_{m=1}^{M} \sqrt{\eta_{mk}} \rho_{mk} \right)^2 \\ &\times \left\{ (1-\theta) P_d \sum_{\substack{k'=1 \\ k' \neq k}}^{K} \left[ \sum_{m=1}^{M} \sqrt{\eta_{mk'}} \rho_{mk'} \frac{\beta_{mk}}{\beta_{mk'}} \right]^2 \left| \boldsymbol{\varphi}_k \boldsymbol{\varphi}_{k'}^{H} \right|^2 \right. \\ &\left. + (1-\theta) P_d \sum_{m=1}^{M} \sum_{k'=1}^{K} \eta_{mk'} \rho_{mk'} \beta_{mk} + 1 \right\}^{-1}. \end{aligned} \tag{15}$$

Then, according to (7), (8) and (15), we can get the achievable data rate and the decoding error probability with $n' = (1-\alpha) n_d$.

### 3.2 Energy Collection

According to reference [9], the collected energy can be modeled as

$$\begin{aligned} EH(P_R) &= \left[ \frac{a}{1-b} \left( \frac{1}{1+\exp\left(-c\left(P_R - d\right)\right)} - b \right) \right]^{+} \\ &= \left[ \frac{a\left(1-\exp\left(-cP_R\right)\right)}{1+\exp\left(-c\left(P_R - d\right)\right)} \right]^{+}, \end{aligned} \tag{16}$$

where $EH(P_R)$ refers to the energy collected instantaneously, $b = 1/(1+\exp(cd))$, $[z]^{+} = \max(0, z)$. According to the literature [8], $a = 20$ mW, $c = 6400/\mu$W, $d = 2.9$ $\mu$W.

**Instantaneous Energy Collection.** Based on TS and PS protocols, the total instantaneous energy $E_k$ collected by the $k$-th UE can be expressed as

$$E_k = \alpha n_d EH\left(P_k\right) + \left(1-\alpha\right) n_d EH\left(\theta P_k\right), \tag{17}$$

where $EH\left(P_R\right)$ represents the energy collected instantaneously [9] and $P_k$ represents the received power of the $k$-th UE. Let $s_k \in \left\{s_k^{(1)}, ..., s_k^{(\tilde{n}_d)}\right\}$, then according to (13), the received power $P_k$ of the $k$-th UE can be expressed as

$$P_k = P_d \left| \sum_{m=1}^{M} \sum_{k'=1}^{K} \sqrt{\eta_{mk'}} g_{mk} \hat{g}_{mk'}^{*} s_{k'} \right|^2. \tag{18}$$

**Average Energy Collection.** The total average energy $\bar{E}_k$ collected by the $k$-th UE can be expressed as

$$\bar{E}_k = \alpha n_d \mathbb{E}\left[EH\left(P_k\right)\right] + \left(1-\alpha\right) n_d \mathbb{E}\left[EH\left(\theta P_k\right)\right]. \tag{19}$$

Since the closed-form expression of (17) is mathematically difficult to calculate, we use Jensen inequality to get an upper bound $\bar{E}_k^{\mathrm{UB}}$ of $\bar{E}_k$, that is

$$\bar{E}_k \leq \bar{E}_k^{\mathrm{UB}} = \alpha n_d EH\left(\mathbb{E}\left[P_k\right]\right) + \left(1-\alpha\right) n_d EH\left(\theta \mathbb{E}\left[P_k\right]\right). \tag{20}$$

Combined with (5), (6), and (18), the derived expression of $\mathbb{E}\left[P_k\right]$ is

$$\begin{aligned}
\mathbb{E}\left[P_k\right] =& P_d \mathbb{E}\left[\left| \sum_{m=1}^{M} \sqrt{\eta_{mk}} g_{mk} \hat{g}_{mk}^{*} \right|^2\right] + P_d \mathbb{E}\left[\left| \sum_{m=1}^{M} \sum_{\substack{k'=1 \\ k' \neq k}}^{K} \sqrt{\eta_{mk'}} g_{mk} \hat{g}_{mk}^{*} \right|^2\right] \\
=& P_d \sum_{m=1}^{M} \eta_{mk} c_{mk}^2 \beta_{mk} \left(2 n_p P_p \beta_{mk} + 1\right) \\
&+ P_d \sum_{m=1}^{M} \sum_{\substack{k'=1 \\ k' \neq k}}^{K} \eta_{mk'} c_{mk'}^2 \beta_{mk} \left(n_p P_p \beta_{mk'} + 1\right) \\
=& P_d \sum_{m=1}^{M} \eta_{mk} \rho_{mk}^2 + P_d \sum_{m=1}^{M} \sum_{\substack{k'=1 \\ k' \neq k}}^{K} \eta_{mk'} \rho_{mk'} \beta_{mk}.
\end{aligned} \tag{21}$$

## 4 Simulation Results and Analysis

In this section, we validate our analysis through simulations. The specific parameters are set as shown in Table 1.

**Table 1.** Simulation parameter settings

| Parameters | Value |
|---|---|
| Number of AP $M$ | [100, 200] |
| Number of UE $K$ | [50, 100] |
| Coherence Bandwidth $B_c$ | 200 kHz |
| Coherence Time $T_c$ | 1 ms |
| Bandwidth $B$ | 20 MHz |
| Transmitting Power of Uplink Pilot $P_p$ | 100 mW |
| Average Transmitting Power of Downlink $p_d$ | [100, 200] mW |
| Decoding Error Probability $\varepsilon_k$ | $10^{-6}$ |
| Path Loss Factor $\alpha_{PL}$ | 3.4 |

Figure 3 shows the relationship between the decoding error probability $\varepsilon_k\,(n_d, \gamma_k)$ and the coding block length $n_d$ for the $k$-th UE. The decoding error probability $\varepsilon_k$ decreases continuously as the coding blocklength $n_d$ keeps increasing in the finite blocklength regime. By comparing the blue ($K = 100$), orange ($K = 75$) and green ($K = 50$) curves, we see that the decoding error probability increases when the number of UE $K$ rises. Therefore, to meet different service requirements, when the number of UE $K$ increases, the coding blocklength $n_d$ can be increased appropriately to keep the reliability within an acceptable range.

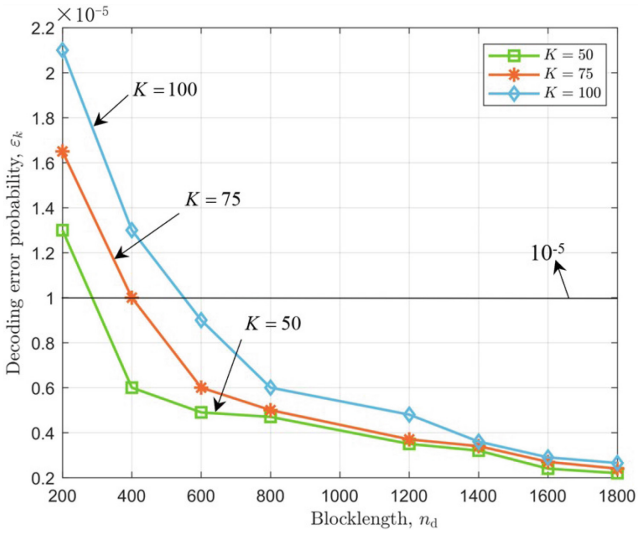


**Fig. 3.** Relationship between error probability $\varepsilon_k$ and blocklength $n_d$.

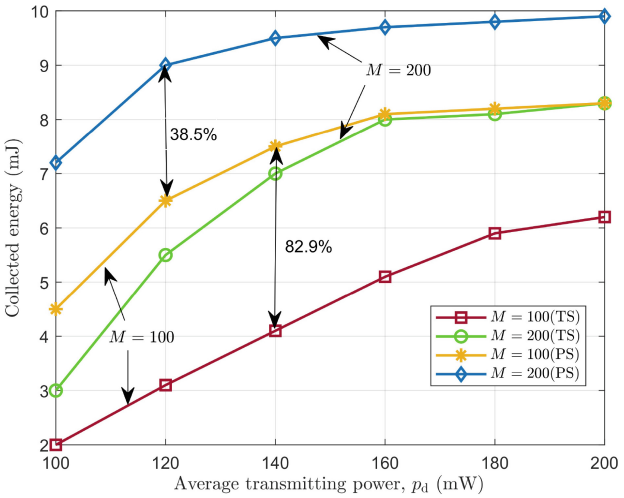


**Fig. 4.** Collected energy versus average transmitting power $p_d$.

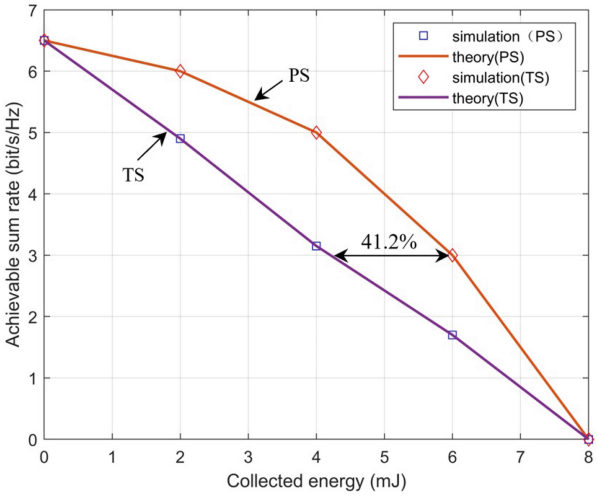


**Fig. 5.** Trade-off between achievable sum rate and collected energy.

Figure 4 plots the relationship between the collected energy and the average transmit power $p_d$, respectively using TS protocol and PS protocol, with $\alpha = 0.5$ and $\theta = 0.5$. As the average transmit power $p_d$ keeps increasing, the energy collected by UE increases accordingly. From the figure, it is obvious that increasing the number of distributed AP can increase the energy collected by the UE regardless of whether TS or PS protocol is used. Specifically, increasing the number of AP from 100 to 200 increases the energy collected by the UE by 38.5

% when the PS protocol is used and the average transmitting power is $p_{\mathrm{d}} = 120$ mW. In addition, the PS protocol is superior to the TS protocol.

Figure 5 depicts the trade-off between achievable rate and collected energy with $M = 100$, $K = 50$, $p_{\mathrm{d}} = 200$ mW and $\alpha = 0$ corresponds to PS protocol and $\theta = 0$ corresponds to TS protocol. When $\alpha$ or $\theta$ tends to 0, the achievable rate will reach its maximum. Meanwhile, the CU allocated for downlink transmission will be used only for data transmission, while the energy collected by UE becomes infinitesimal. When $\alpha$ or $\theta$ converges to 1, the energy collected by UE reaches the maximum, CU allocated for downlink transmission is only used for energy transmission and the achievable rate of UE becomes infinitesimal. Therefore, by adjusting the value of TS factor $\alpha$ or PS factor $\theta$, the compromise curve in Fig. 5 can be traversed to meet different rate-energy requirements.

## 5 Conclusion

In this paper, we have proposed a performance analysis and optimization strategy over CF mMIMO for short packet transmission. The main steps of the strategy are expected to support mURLLC with ultra-high energy or spectral efficiency in the future. Furthermore, we have combined CF mMIMO with SWIPT to derive the SINR and energy collected under imperfect CSI. At the same time, combined with FBL information theory, the downlink achievable data rate and error probability have been deduced. The simulation results have shown the correlation between performances and that CF mMIMO can improve the system performance, which has verified the effectiveness of the proposed strategy.

## References

1. Elhoushy, S., Ibrahim, M., Hamouda, W.: Cell-free massive MIMO: a survey. IEEE Commun. Surveys Tutorials **24**(1), 492–523 (2021)
2. Liu, Y., Deng, Y., Elkashlan, M., Nallanathan, A., Karagiannidis, G.K.: Optimization of grant-free noma with multiple configured-grants for mURLLC. IEEE J. Sel. Areas Commun. **40**(4), 1222–1236 (2022)
3. Marzetta, T.L., Yang, H.: Fundamentals of massive MIMO. Cambridge University Press (2016)
4. Nasir, A.A., Tuan, H.D., Ngo, H.Q., Duong, T.Q., Poor, H.V.: Cell-free massive MIMO in the short blocklength regime for URLLC. IEEE Trans. Wireless Commun. **20**(9), 5861–5871 (2021)
5. Ngo, H.Q., Ashikhmin, A., Yang, H., Larsson, E.G., Marzetta, T.L.: Cell-free massive MIMO versus small cells. IEEE Trans. Wireless Commun. **16**(3), 1834–1850 (2017)
6. Polyanskiy, Y., Poor, H.V., Verdú, S.: Channel coding rate in the finite blocklength regime. IEEE Trans. Inf. Theor. **56**(5), 2307–2359 (2010)
7. Saad, W., Bennis, M., Chen, M.: A vision of 6G wireless systems: Applications, trends, technologies, and open research problems. IEEE Network **34**(3), 134–142 (2020). https://doi.org/10.1109/MNET.001.1900287
8. Steven, M.K.: Fundamentals of statistical signal processing. PTR Prentice-Hall, Englewood Cliffs, NJ **10**, 151045 (1993)

9. Wang, S., Xia, M., Huang, K., Wu, Y.C.: Wirelessly powered two-way communication with nonlinear energy harvesting model: Rate regions under fixed and mobile relay. IEEE Trans. Wireless Commun. **16**(12), 8190–8204 (2017)
10. You, X., et al.: Towards 6G wireless communication networks: Vision, enabling technologies, and new paradigm shifts. SCIENCE CHINA Inf. Sci. **64**(1), 1–74 (2021)
11. Zhang, X., Wang, J., Poor, H.V.: Statistical delay and error-rate bounded QoS provisioning for mURLLC over 6G CF M-MIMO mobile networks in the finite blocklength regime. IEEE J. Sel. Areas Commun. **39**(3), 652–667 (2020)
12. Zhang, X., Wang, J., Poor, H.V.: Statistical delay and error-rate bounded QoS provisioning for SWIPT over CF M-MIMO 6G mobile wireless networks using FBC. IEEE J. Selected Topics Signal Process. **15**(5), 1272–1287 (2021)